Supporting Information

Simultaneous Enhancements of UV-Shielding Properties and Thermal-/Photo-stability of PVC via Incorporation of Defect-Rich CeO_2 Nanoparticles

Zequan Hu,[a] Si Wang,[a] Xin Zhang,[a] Guoli Fan,[*,a] Yingdi Lv,[b] Xiaodong Zheng,[*,b] Lan Yang,[a] Feng Li[*,a,c]

[a.] State Key Laboratory of Chemical Resource Engineering, Beijing University of Chemical Technology, Beijing, 100029, P.R. China.

[b.] Xi'an Modern Chemistry Research Institute, Xi'an, Shaanxi 710065, P.R. China

[c.] Beijing Advanced Innovation Center for Soft Matter Science and Engineering, Beijing University of Chemical Technology, Beijing 100029, P.R. China.

* To whom all correspondence should be addressed

Tel.: 8610-64451226; Fax: 8610-64425385.

E-mail: fangl@mail.buct.edu.cn (G. Fan);

zxd2046@126.com (X. Zheng);

lifeng@mail.buct.edu.cn (F. Li)

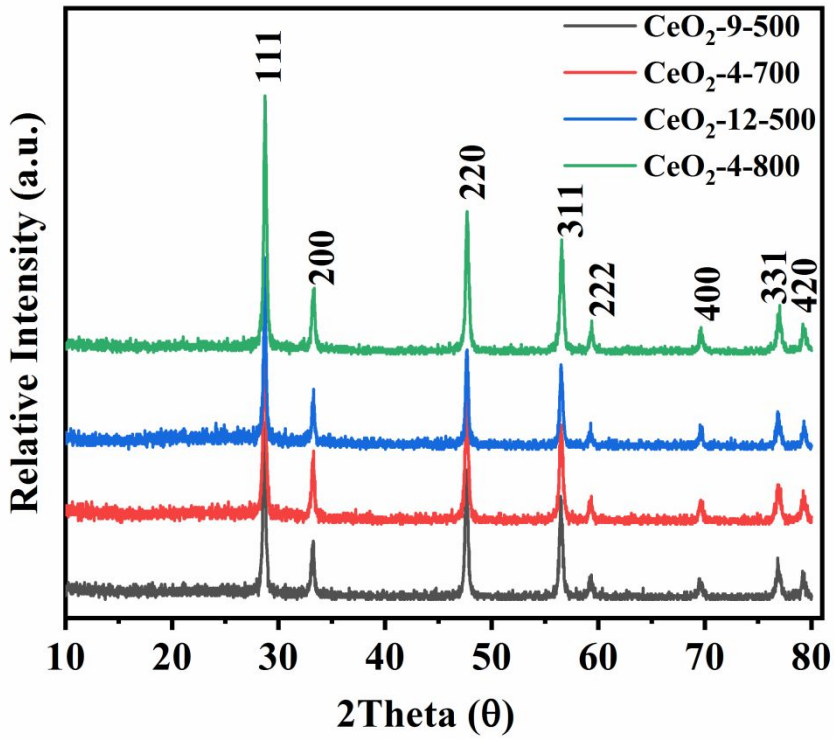

Figure S1 XRD patterns of different CeO_2 powder samples.

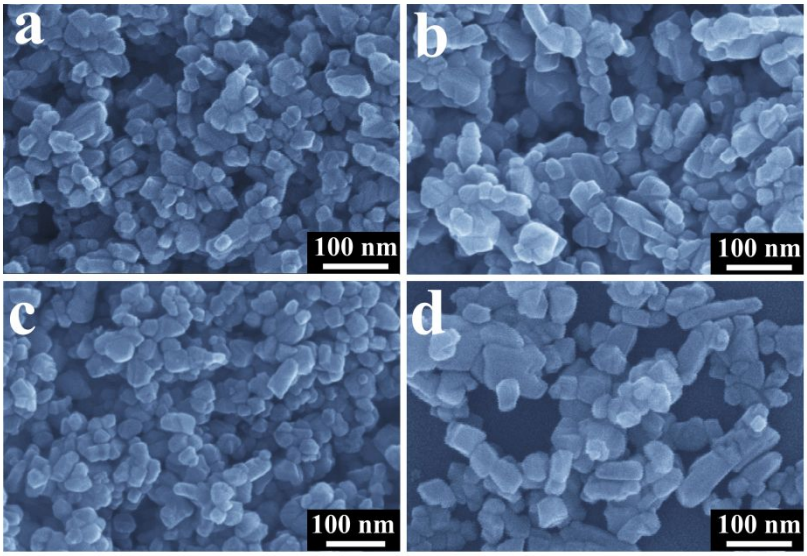

Figure S2 XRD patterns of different CeO_2 samples: (a) CeO_2-9-500, (b) CeO_2-12-500, (c) CeO_2-4-700, and (d) CeO_2-4-800.

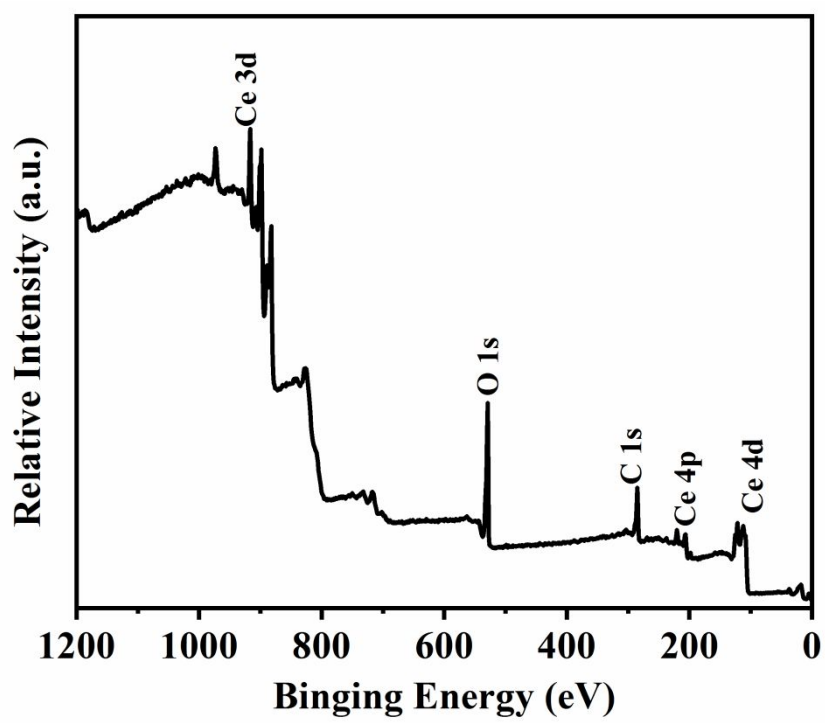

Figure S3 Representative XPS survey of CeO_2-4-500 nanoparticle.

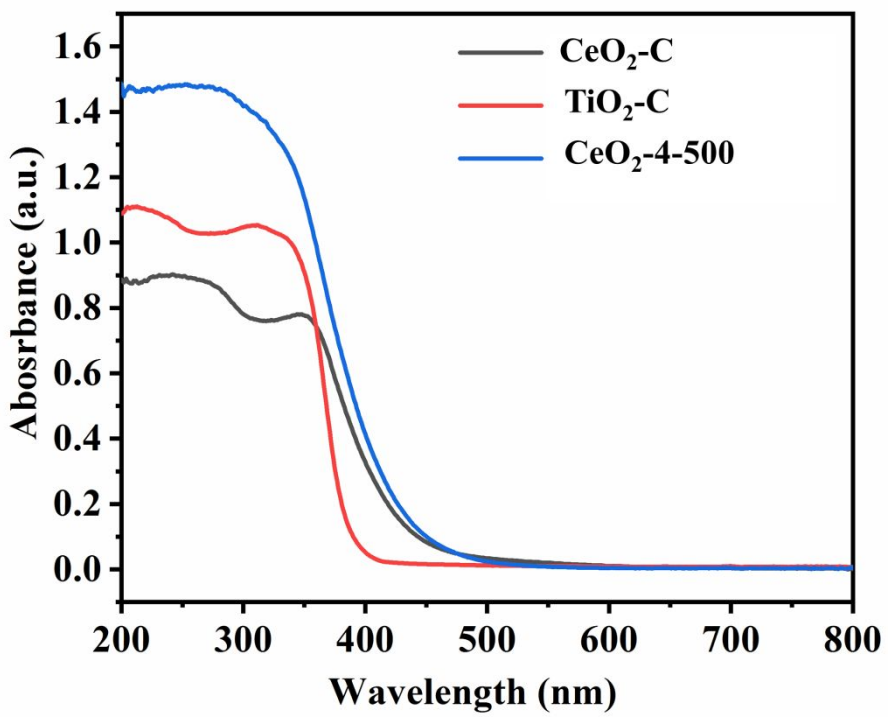

Figure S4 UV-vis absorption spectra of different powder samples.

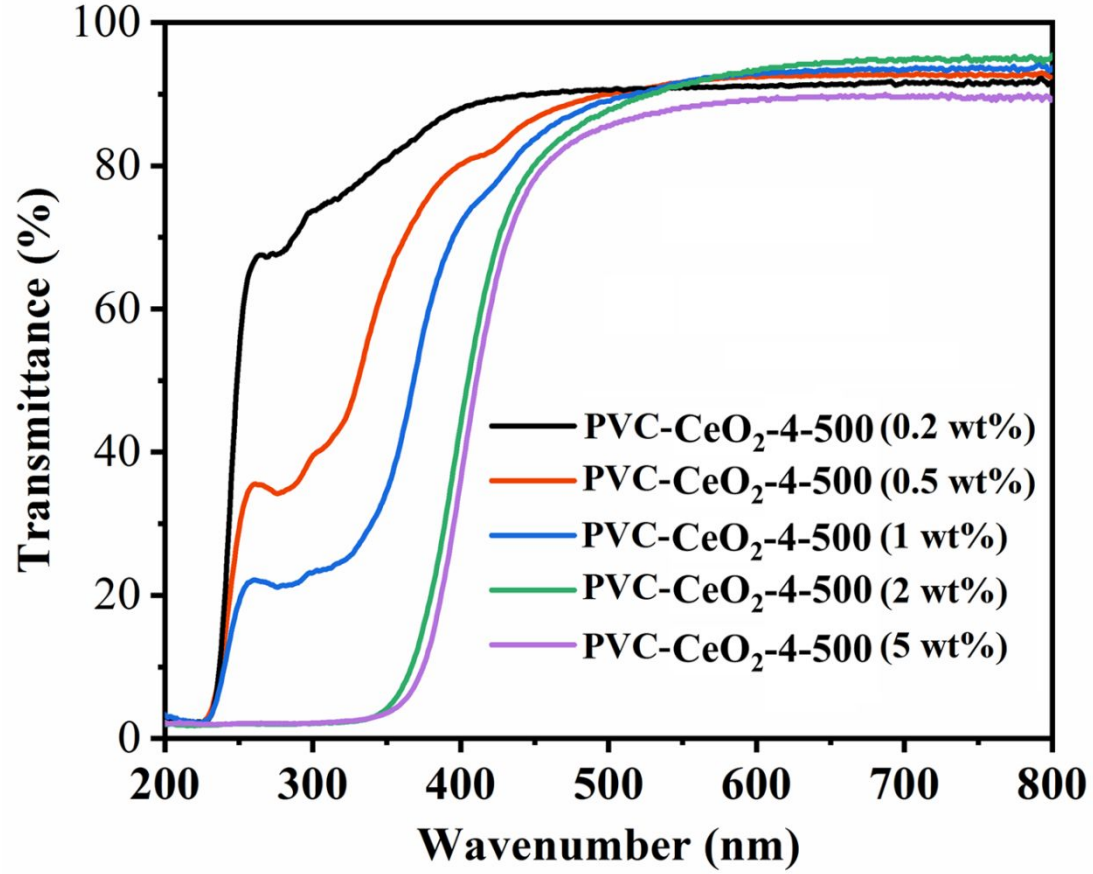

Figure S5 UV-vis light transmittance spectra of PVC-CeO_2-4-500 composite films with different CeO_2-4-500 content.

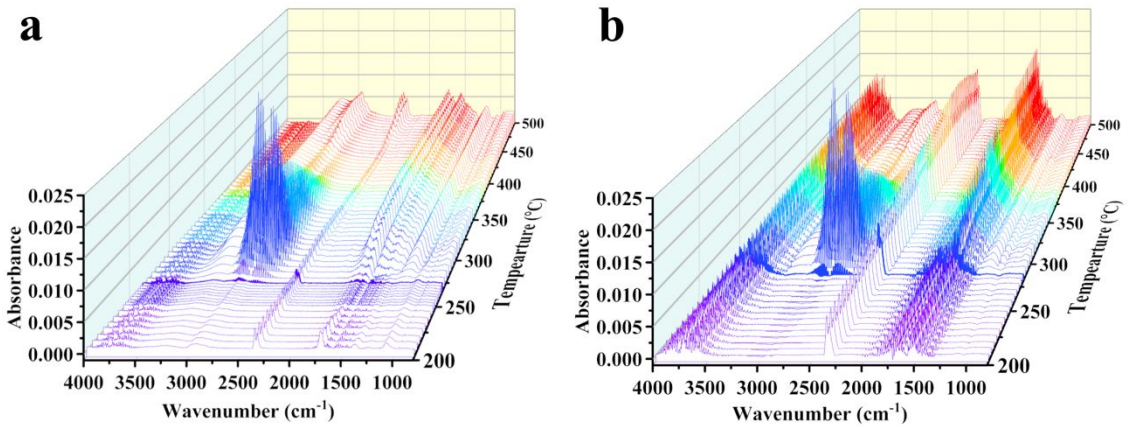

Figure S6 3D-FTIR spectra of the evolved gaseous of (a) pristine PVC and (b) PVC-CeO_2-4-500 film under different pyrolysis temperatures.

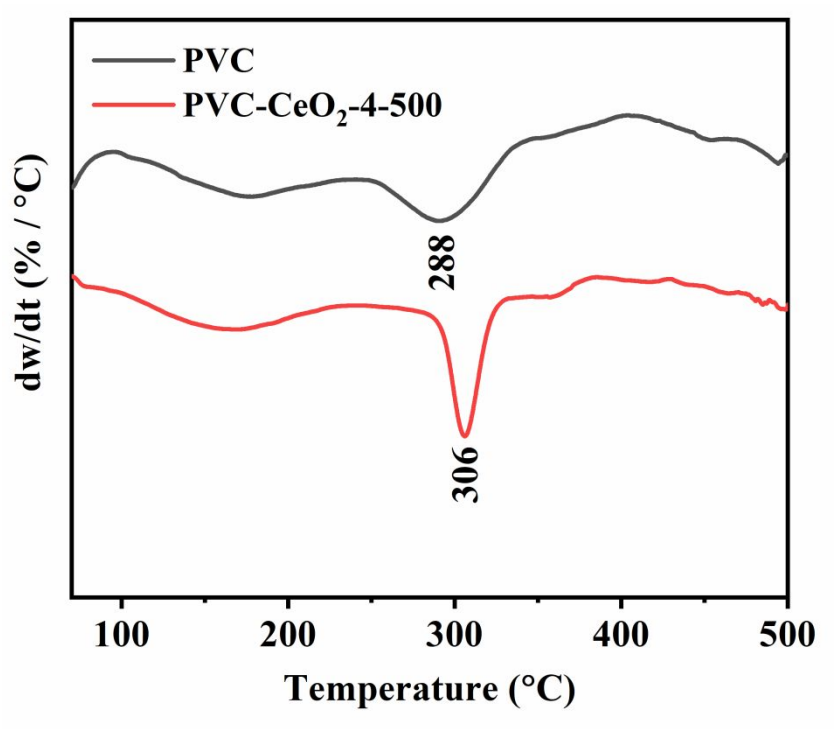

Figure S7 DTG curves of PVC and PVC-CeO_2-4-500 composite film.

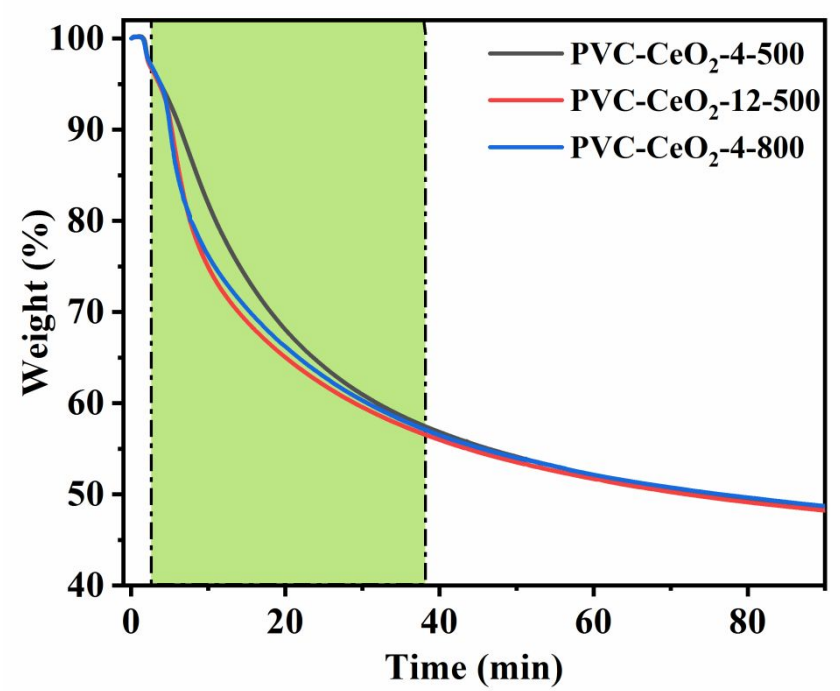

Figure S8 Isothermal TG of the PVC-CeO_2 composite films with different CeO_2 powder sample.

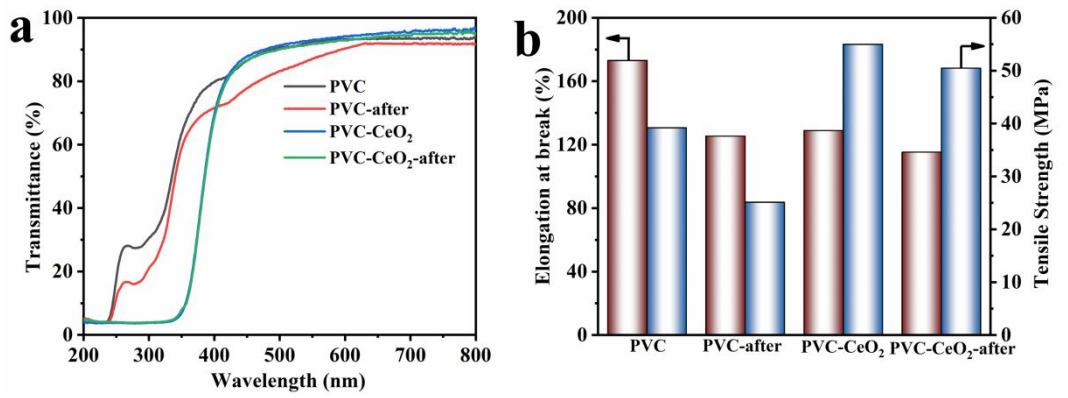

Figure S9 (a) UV-vis light transmittance spectra and (b) tensile strength and elongation at break of PVC and PVC-CeO_2 composite film (with 2wt% CeO_2-4-500) before and after UV irradiation.

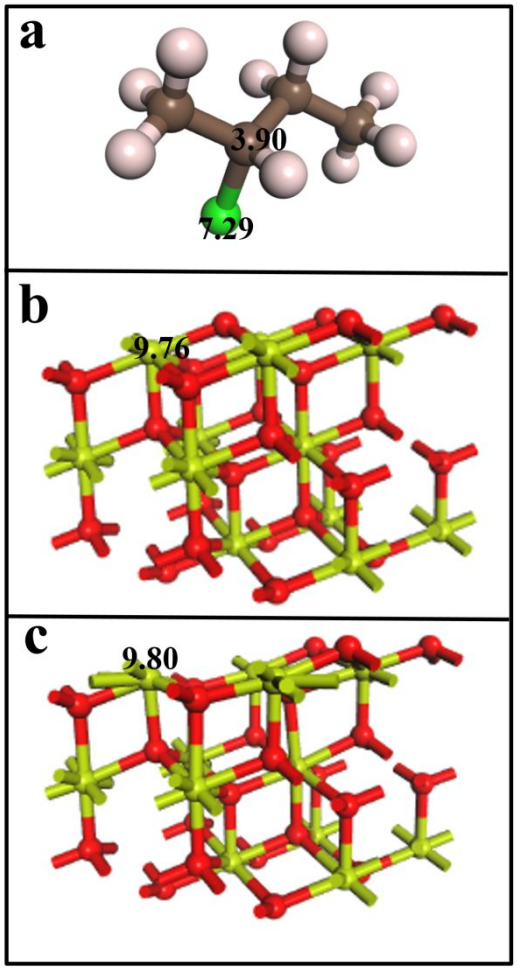

Figure S10 Optimized structure of (a) free 2-chlorobutane molecular, (b) clean stoichiometric CeO_2 (111) surface, and (c) clean defect-rich CeO_2 (111) surface